Buckling of monopod bucket foundations—influence of boundary conditions and soil–structure interaction

Søren Madsen[*1], Rodney Pinna[2], Mark Randolph[3] and Lars V. Andersen[1]

[1]*Department of Civil Engineering, Aalborg University, Sofiendalsvej 9-11, DK-9000 Aalborg, Denmark*
[2]*AkerSolutions Pty. Ltd., Perth, Western Australia, Australia*
[3]*Centre for Offshore Foundation Systems, The University of Western Australia, 35 Stirling Highway, CRAWLEY WA 6009, Australia*

Abstract. Using large monopod bucket foundations as an alternative to monopiles for offshore wind turbines offers the potential for large cost savings compared to typical piled foundations. In this paper, numerical simulations are carried out to assess the risk of structural buckling during installation of large-diameter bucket foundations. Since shell structures are generally sensitive to initially imperfect geometries, eigenmode-affine imperfections are introduced in a nonlinear finite-element analysis. The influence of modelling the real lid structure compared to classic boundary conditions is investigated. The effects of including soil restraint and soil–structure interaction on the buckling analysis are also addressed.

Keywords: monopod; bucket foundation; buckling; instability

1. Introduction

The installation concept of the monopod bucket foundation is similar to that of the well-proven suction anchor or suction caisson, but the forces carried during operation are different from those on a suction caisson. The suction caisson is loaded mainly by uniaxial forces, whereas the loads from the wind on the wind turbine and the wave loads result in a large overturning moment—in shifting directions—on the bucket foundation (Houlsby *et al.* 2005, Ibsen 2008). The loads on the monopod bucket are accommodated by a combination of earth pressures on the bucket skirt and the vertical bearing capacity of the bucket.

Installation of a bucket foundation requires minimal installation equipment since it is installed by a combination of water evacuation from the cavity between the bucket lid and the soil seabed and water injection at the skirt tip. Pumping out water is causing the bucket foundation to be loaded by hydrostatic pressure (internal suction). The suction introduces a pressure differential across the bucket lid, which increases the downward force on the bucket lid. At the same time, the water flow reduces the effective stresses around the skirt tip and the penetration resistance is reduced. Furthermore, at the end of the life of the supported structure, the bucket foundation can be removed by applying pressure instead of suction. This has been tested in the laboratory and at a

---

large-scale test facility in Frederikshavn, Denmark, where several buckets were installed by suction, loaded and finally removed by overpressure (Ibsen 2008).

In the initial installation phase, the free height of the skirt above the seabed is large, and a low suction pressure is needed to overcome the soil resistance. For subsequent installation phases, a larger pressure is required. The penetration resistance of skirted foundations has been investigated by for example Tjelta (1995), Andersen *et al*. (2008), Tran and Randolph (2008), and Ibsen and Thilsted (2010). Simultaneously, during installation the degree of skirt fixation increases due to the lateral restraint offered by the surrounding soil. The lateral restraint provided by the soil to the embedded skirt may increase the buckling loads significantly. No current design codes provide guidance on the use of the surrounding soil to provide restraint against buckling.

The geometry of the bucket foundation is basically a thin shell structure with a relatively large aspect ratio between the skirt diameter and the wall thickness (typically $r/t > 200$). The combination of a thin shell structure and suction forces makes the structure prone to buckling during the installation process. Several analytical expressions for the structural buckling pressure of circular cylindrical shells exist; cf. e.g., (Brush and Almroth 1975, Farshad 1992). These analytical eigenvalue solutions do not account for imperfections of the initial geometry but assume a perfect circular cylindrical shape for the structure.

However, the collapse load of cylindrical shells is known to be sensitive to the presence of initial imperfections and the effects of imperfections must be considered to arrive at accurate predictions of cylinder buckling loads. Detailed reviews of the imperfection sensitivity of cylinders are provided in Bushnell (1981), Simitses (1986), Noor (1990), and Teng (1996). It is well established that cylinders under axial compression show large imperfection sensitivity while those under lateral or hydrostatic loading show a smaller degree of sensitivity. The influence of imperfections is commonly accounted for by the use of a "knockdown factor" which is a multiplier applied to the eigenvalue buckling solution.

For cylinders under lateral or hydrostatic load, typical knockdown factors are in the range of 0.6 (Odland and Faulkner 1981, DNV-RP-C202) to 0.78 (NASA 1968). The current Eurocode (EN 1993-1-6) includes a range of knockdown factors dependent on the fabrication quality, ranging from 0.5 to 0.75 for elastic buckling. Further corrections are available to account for plasticity effects.

Knockdown factors are applied to linear bifurcation solutions. As an alternative to this procedure, a fully nonlinear analysis can be undertaken. Recent work has shown that when imperfection patterns are known, this method is able to produce accurate prediction of buckling and collapse loads (de Paor *et al*. (2012), for example). For newly fabricated cylinders however, it is impossible to know the shape and size of any initial imperfections. This is particularly the case where a small number of such cylinders are being fabricated as is typical in the offshore construction industry. Hence, it is necessary to use a method of specifying an equivalent imperfection to account for their effect.

While the need to include the effects of imperfections is well known, there is no well-defined procedure in the literature to account for these effects. Typical proposals are to use a realistic imperfection based on the known manufacturing procedure, see e.g., (Arbocz 1982) as cited by (Schmidt 2000), or to use an imperfection of the same shape as the eigenmode (EN 1993-1-6, Prabu *et al*. 2009). Other methods include the use of an equivalent load to provoke buckling (Haynie *et al*. 2010) or an imperfection in the shape of a dent or some other pattern (Guggenberger 1995, Hrinda 2012). None of these methods has been shown to provide a guaranteed lower bound. Generally, this work has shown that for laterally loaded cylinders, a buckling mode in the shape of

an eigenmode provokes the lowest buckling mode; this is also the default in the Eurocode (EN 1993-1-6). Often the imperfection applied is in the shape of the lowest eigenmode. However, recent work (Madsen *et al*. 2013) has shown that lower collapse loads can be obtained by applying a higher buckling mode, depending on the magnitude of the imperfection.

When cylindrical shell structures are designed according to standards such as, for example, DNV (DNV-RP-C202) or Eurocode (EN 1993-1-6), assumptions of idealized boundary conditions (pinned, fixed or free) must be made. None of the design regulations accounts for the lateral restraints offered by the surrounding soil. Recently, this lateral restraint offered by the soil has been modelled by radial elastic Winkler springs (Pinna and Ronalds 2000, Lee and Tran 2013, Hanssen *et al*. 2013) or Pasternak type foundations (Sofiyev 2010). Pinna and Ronalds (2000) considered eigenvalue buckling only and found a simple multiplier that can be applied to the buckling load for a pinned-pinned shell when the amount of lateral restraint is known, and thus obtain intermediate solutions between the pinned and free case. Sofiyev (2010) has investigated the buckling analysis of functionally-graded-material (FGM) circular truncated conical and cylindrical shells subjected to combined axial loads and hydrostatic pressure and resting on a Pasternak type elastic foundation.

Neither of the above-mentioned analyses takes the lateral restraints offered by the soil into account by means of advanced nonlinear finite element solutions. It may be beneficial to perform refined analyses with boundary conditions that are more realistic and with the soil modelled as a continuum. An attempt to do so was reported by Pinna *et al*. (2001) for suction caissons in clay where the conclusion was:

"In general, it seems prudent to neglect any lateral soil restraint, and to design the caisson shell alone to withstand the applied suction loads."

The soil was modelled by both an elastic model and an elastoplastic Tresca model. However, idealized assumptions of the boundary conditions were still made at the skirt and at the connection to the lid. Further, the soil parameters studied corresponded to weak soils not suited for monopod foundations for wind turbines. In part, this conclusion was motivated by the difficulty in identifying suitable soil stiffness parameters. However, it is believed that the conclusions from these studies of buckling of suction caissons cannot be transferred directly to monopod bucket foundations for offshore wind turbines, where relatively strong soils are usually present and it is believed that the buckling behaviour will resemble the buckling of a pinned-pinned cylinder of length equal to the free height of the partially submerged bucket.

In this paper, the hydrostatic bucking load is assessed by numerical analysis in ABAQUS. Both linear eigenvalue buckling analysis and nonlinear buckling analysis considering material plasticity and eigenmode-affine imperfections are executed. In Section 3, the effect of modelling the real bucket lid structure is compared to idealized boundary conditions. In Section 4, the soil restraint is investigated using more representative soil parameters for a wind turbine location and the influence of the soil–structure interaction properties on the buckling load is investigated through the use of a contact based analysis. In the knowledge of the authors, no previous attempts have been made to investigate the influence of the soil–structure interaction properties on the buckling load. In Section 3, the bottom of the cylinder is considered pinned and various cylinder lengths are considered. Conversely, the bottom of the cylinder is unconstrained (except for the soil–structure interaction) in Section 4 where the cylinder length is kept constant but the penetration ratio is varied.

2. Material and methods

In the comparative study of buckling loads for the monopod bucket, four kinds of boundary conditions are considered regarding the top of the skirt:

- Pinned, also known as the "classical", boundary condition S_3: The end displacements are axially free but circumferentially restrained in-plane (zero radial and tangential deflection). This makes the end free to warp. S_3S_3 boundary conditions are illustrated in Fig. 1. Also shown in Fig. 1 are the two load cases: Lateral pressure ($P = 0$) and hydrostatic pressure ($P = qr^2\pi$).
- Clamped (C_3): The end displacements are axially free but circumferentially restrained in-plane as for the pinned boundary condition. In addition, the rotation is restrained. This hinders the end from warping.
- Fully clamped (C_4): All rotations and displacements are set to zero.
- Physical model of the lid (Lid): The lid structure is modelled by a steel plate twice as thick as the skirt and with 12 stiffening ribs, as shown in Fig. 2(a). The diameter of the shaft is half the bucket diameter. This is a typical arrangement for a wind-turbine monopod foundation.
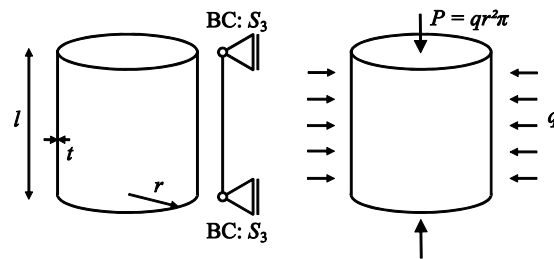

Fig. 1 Left: Shell dimensions and illustration of S_3S_3 boundary conditions. Right: Illustration of lateral pressure ($P = 0$) and hydrostatic pressure ($P = qr^2\pi$)

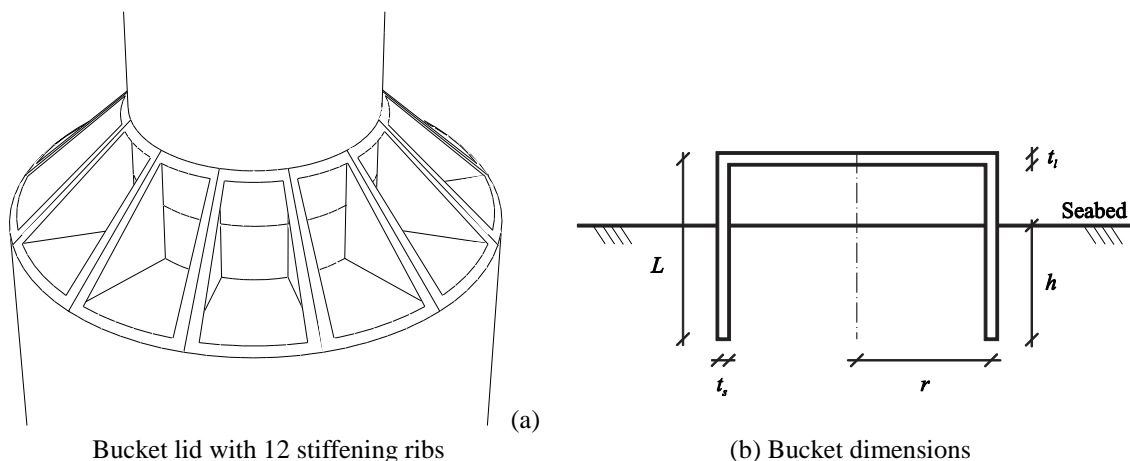Bucket lid with 12 stiffening ribs   (b) Bucket dimensions

Fig. 2 Bucket lid and dimensions

For the bottom of the cylinder i.e. the tip of the skirt, two types of constraints are analysed:
- Pinned (S_3) where it is expected that the soil restraint will provide a response similar to the pinned case.
- Soil coupling (soil) when the soil restraint is modelled by elastic continuum elements at the submerged part of the skirt. No further constraints are applied to the bottom of the cylinder in this case.

2.1 Material properties

The bucket foundation is made of steel with a Young's modulus of $E = 210$ GPa, a Poisson's ratio of $v = 0.3$, and an initial yield stress of $\sigma_{y0} = 235$ MPa. The elastic properties of the surrounding soil are defined by Poisson's ratio $v_{soil} = 0.25$ and Young's modulus $E_{soil} = 25$ MPa. The Young's modulus for the soil is chosen as a lower value for sand at a typical wind turbine location where a monopod bucket foundation could be considered (see e.g., (Andersen 2010) or (Lesny 2010)). Soil plasticity is not relevant for soil parameters typical for monopod foundations according to Fig. 3 from Pinna (2004) where no plastic zones are observed for $s_u = 50$ kPa and $E_{soil} = 5$ MPa.

$E_{soil}/s_u = 100$; $s_u = 50$ kPa
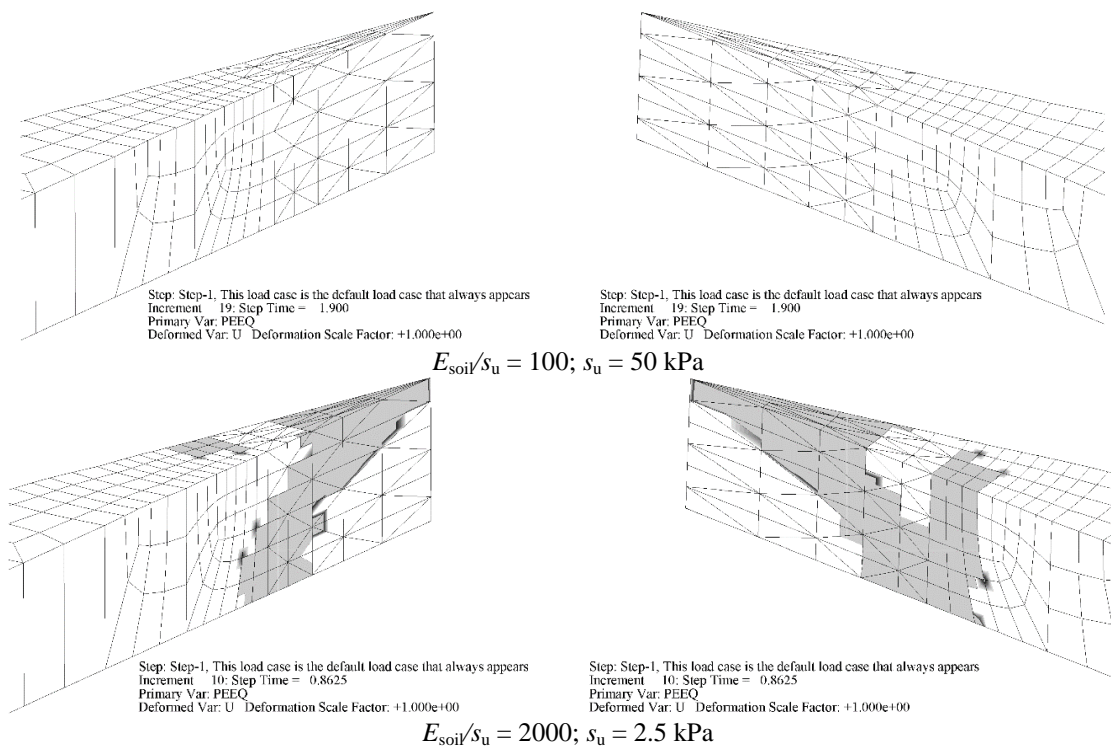
$E_{soil}/s_u = 2000$; $s_u = 2.5$ kPa

Fig. 3 Extent of plastified zone in the soil for a fully embedded S_3S_3 cylinder at maximum load. The grey zones indicate plasticity. The view is cut horizontally at the plane of symmetry and shows $z/L = 0.5$ to 1.0, i.e., line of q symmetry at top, pinned support at bottom. $E_{soil} = 5$ MPa. The shell is located at the point where the mesh changes from tetrahedral to hexahedral elements. Figure from (Pinna 2004)

(a) Hydrostatic loading of partially submerged cylinder

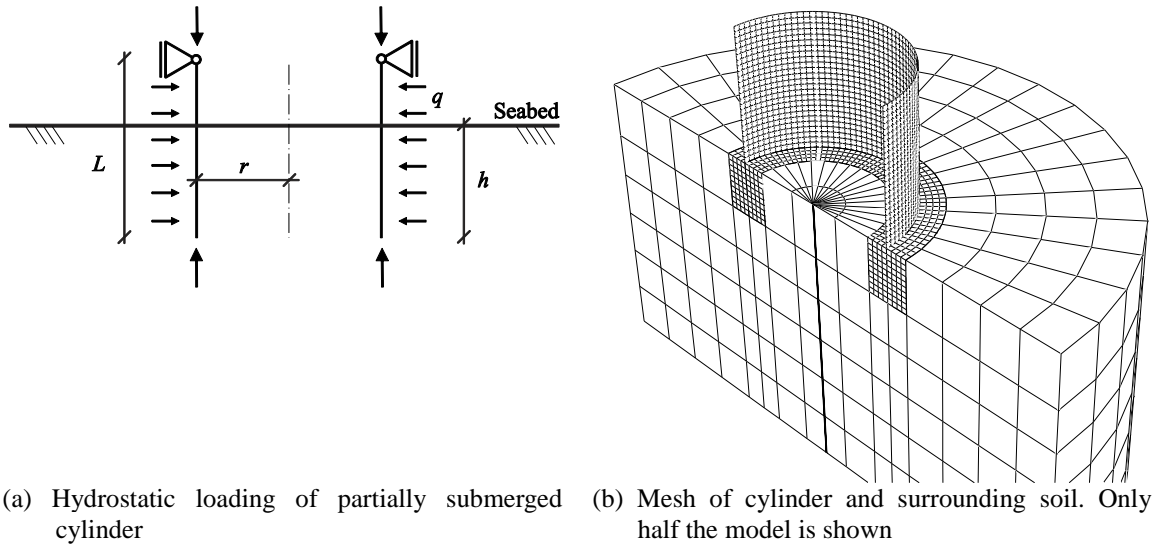(b) Mesh of cylinder and surrounding soil. Only half the model is shown

Fig. 4 Loading and mesh of partially submerged cylinder as used in Section 4

In this work, it was found that for soils with high s_u/E_{soil} ratios the surrounding material remained elastic at the point of collapse of the cylinder. Conversely, for soils with low s_u/E_{soil} ratios, failure of the shell and soil system occurred when a fully plastic zone was able to form within the soil.

2.2 Numerical buckling analysis

The finite element package ABAQUS is used for the numerical analysis. The steel is modelled as a linear elastic–perfect plastic material with yielding defined by the von Mises yield criterion. The bucket foundation is modelled using 8-noded quadrilateral shell elements with quadratic interpolation and reduced integration (S8R). The surrounding soil is modelled using 8-noded solid elements with linear spatial interpolation and reduced integration (C3D8R). For the soil, "near-field elements" are added. These near-field elements have the same properties as the rest of the surrounding soil, but the mesh size matches that of the shell elements applied for the bucket skirt. The near-field soil elements are employed within a zone that reaches 1 m away from the skirt (inside as well as outside) and 2 m below the skirt tip. The mesh of the bucket and the surrounding soil is shown in Fig. 4.

When the surrounding soil is included (Section 4), the shell elements of the bucket are coupled to the solid elements of the soil in two different ways:

- Tie constraints that fuse the surfaces of two regions together, even though they have dissimilar meshes and different degrees of freedom. Tie constraints are also used to couple the near-field soil elements to the surrounding soil. The tie constraint ties each node on the slave surface to the closest master surface so there is no relative motion between them. In the initial phase of the analysis, the initial position of the slave surfaces is adjusted so all nodes of the slave surfaces are moved onto the master surface. The tie constraints represent

- some simplification to the true soil–structure interaction where the bucket skirt interacts with the surrounding soil by frictional contact.
- In an attempt to model the soil–structure interface more realistically, the tangential behaviour of the interface is modelled by Coulomb friction $\tau = \mu p$, where τ is the interface shear stress, $\mu = \tan \delta$ is the friction coefficient, and p is the normal stress in the interface. Friction coefficients of 0.42 and 20 are used. A friction coefficient of 0.42 corresponds to an interface friction angle of $\delta = 23°$ which is considered as a realistic conservative estimate of true soil–structure behaviour between sand and steel. The friction coefficient of 20 is an unrealistically high value chosen to represent no sliding. The normal behaviour is modelled with a high-penalty overlap stiffness, corresponding to "hard" contact, and separation is allowed.

The numerical buckling analysis is made in two steps. Step 1 is a linear eigenvalue buckling analysis used to find an estimate of the initial imperfect geometry based on buckling mode shapes (eigenvectors). A linear prediction of the buckling load (eigenvalue) is also found in Step 1. The Lanczos Eigensolver is used to extract the eigenvalues in this analysis. Step 2 is a nonlinear analysis where an imperfection in the geometry is introduced by adding the buckling mode shapes determined in step one to the "perfect" geometry. The imperfection has the form

$$\Delta_i = \sum_{i=1}^{M} w_i \psi_i \tag{1}$$

where ψ_i is the ith mode shape (maximum nodal displacement normalised to 1) and w_i is the imperfection scale factor. In the rest of this paper, the magnitude of the imperfections is measured relative to the skirt thickness ($w_0{}^* = w_i/t_s$).

For each penetration depth, the linear buckling mode shape corresponding to a certain penetration depth is introduced as an imperfection. Thus, the imperfect geometry is different for each penetration depth. A uniformly distributed hydrostatic pressure is applied incrementally, and the buckling load is determined as the load level where no further strain energy can be accumulated. Yielding of steel is allowed, i.e. failure is not defined by initial yielding.

3. Buckling of a cylinder with one end pinned and various boundary conditions at the other end

The geometry of the bucket cylinder can be described by the non-dimensional Batdorf parameter

$$Z = \frac{l^2}{rt} \sqrt{1 - v^2}, \tag{2}$$

where l is the height of the (non-embedded) cylinder, identical to l in Fig. 2(b) and L in Fig. 4(a). The shell thickness, t, is that of the cylinder (t_s in Fig. 2(b)). Similarly, a non-dimensional measure of the buckling load is introduced in the form

$$q_{cr}^* = \frac{l^2 r}{\pi^2 D_s} q_{cr},$$ (3)

where the shell bending stiffness is given by

$$D_s = \frac{Et^3}{12(1-v^2)}.$$ (4)

In this paper the buckling load is illustrated by the multiplier α which describes the buckling load relative to the lower-bound approximation, β, for the hydrostatic buckling load of an S_3S_3 cylinder (Odland 1981)

$$\beta = 2\sqrt{1 + \frac{8Z}{3\pi^2}}.$$ (5)

Hence, the buckling load is given by

$$q_{cr}^* = \alpha\beta.$$ (6)

3.1 Eigenvalue buckling (LBA)

In Fig. 5 the buckling load is shown as function of the Batdorf parameter for various boundary conditions. For the fully clamped–pinned (C_4S_3) as well as the pinned–pinned (S_3S_3) case, the results match the findings from Pinna *et al.* (2000) shown in dotted lines. As expected, the Lid–S_3 case (taking $t_l/t_s = 2$) yields results between C_4S_3 and S_3S_3. For Z approaching to zero (a short skirt length) the Lid–S_3 case goes towards the C_4S_3 case.
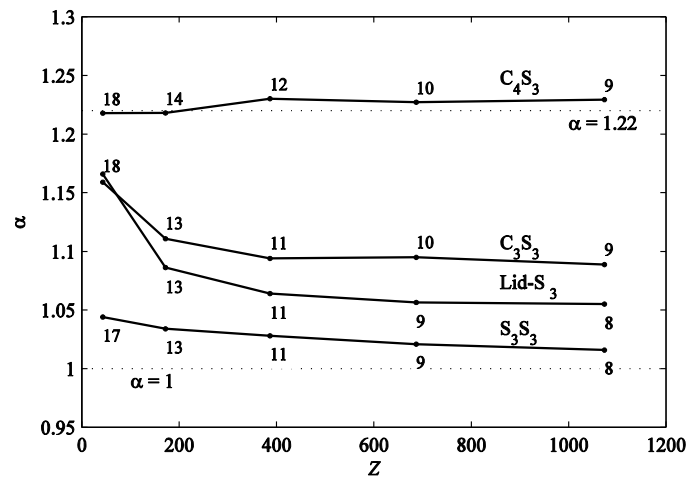

Fig. 5 Linear buckling load for various boundary conditions. Numbers indicate the number of circumferential lobes n in the first buckling mode. For Lid–S_3: $t_l/t_s = 2$
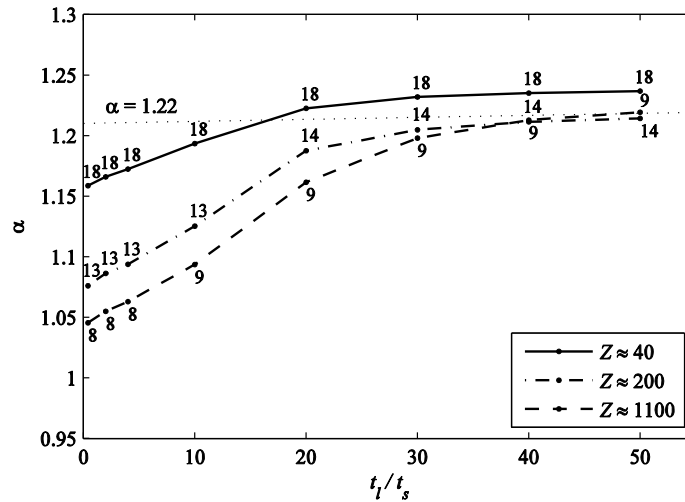
Fig. 6 Linear buckling load as function of lid thickness. The lid has 12 stiffeners. Numbers indicate the number of circumferential lobes n in the first buckling mode
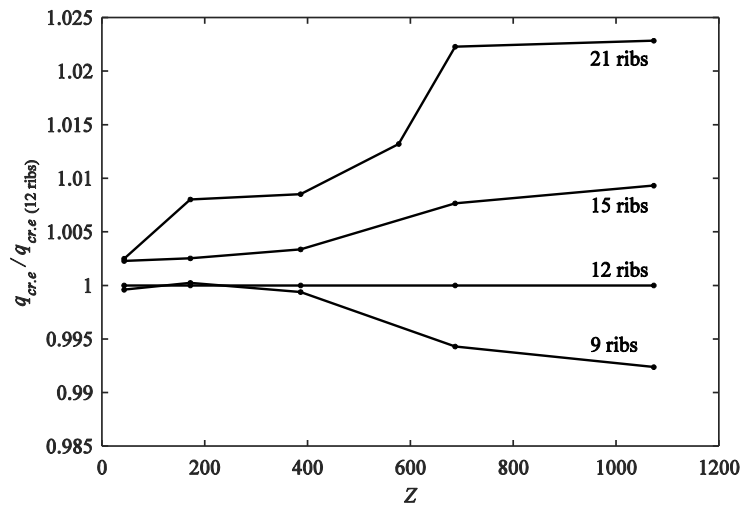

Fig. 7 Linear buckling load for various number of stiffening ribs: $t_l/t_s = 2$

From Fig. 6, where the lid thickness is varied, it can be seen that an equivalent clamped–pinned (C_3S_3) buckling load is reached for $t_l/t_s \approx 40$, corresponding to a staggering lid thickness of one meter for a wall thickness of 25 mm. This is of course a very unrealistic lid thickness. Further, it should be noted that using shell elements for such thick plates might lead to rather unrealistic results for the connection between the skirt and lid. However, this does not change the overall

conclusion—that for a more realistic plate thickness, the lid structure cannot be expected to provide a clamped support at the skirt top.

Finally, the number of stiffeners attached to the lid has been varied between 9 and 21. From Fig. 7 it can be concluded that increasing or decreasing the number of stiffening ribs has almost no influence on the eigenbuckling load.

3.2 Nonlinear buckling with imperfect geometry (GMNIA)

In Fig. 8, the nonlinear hydrostatic buckling load is shown as a function of the varying imperfection amplitude for five different geometries and four different boundary conditions.
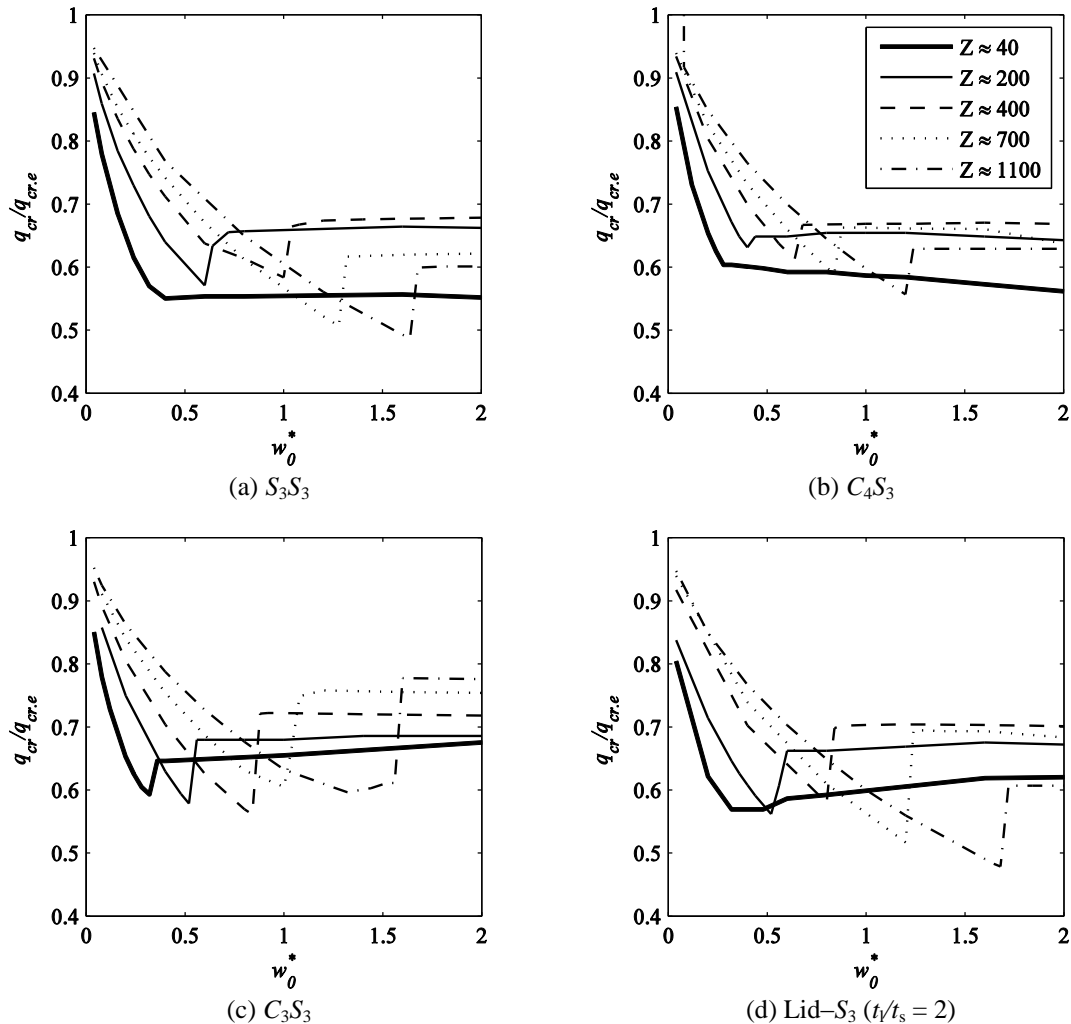

Fig. 8 Critical buckling load normalised by eigenvalue buckling load as a function of imperfection size for various boundary conditions

The amplitude of the critical imperfection varies with the cylinder length. Thus for higher Z values (long cylinders) the critical imperfection amplitude leading to the lowest buckling load becomes even larger than the wall thickness. For example for the S_3S_3 case shown in Fig. 8(a) the critical imperfection amplitude is approximately $w_0^* = 1.3$ for $Z = 700$. For imperfections smaller than the critical imperfection amplitude, the collapse is elastic, while for imperfections larger than the critical imperfection amplitude, the distribution of stresses change, since yielding is allowed, and a higher collapse load can be obtained. The knockdown factors shown in Fig. 8 are 0.48–0.63, so at the lower end of the typical knockdown factors of 0.6 for hydrostatic loading. However, the imperfection reduction factor provided in Eurocode 1993-1-6 for the worst fabrication tolerance is 0.5, which is in good agreement with the obtained results. Generally, higher Z values lead to lower knockdown factors. This trend is also observed in Fig. 9, where the buckling load is illustrated in terms of the multiplier α as function of the Batdorf parameter Z. For higher Z the Lid–S_3 goes towards S_3S_3, so the longer the cylinder the less effect from the lid.
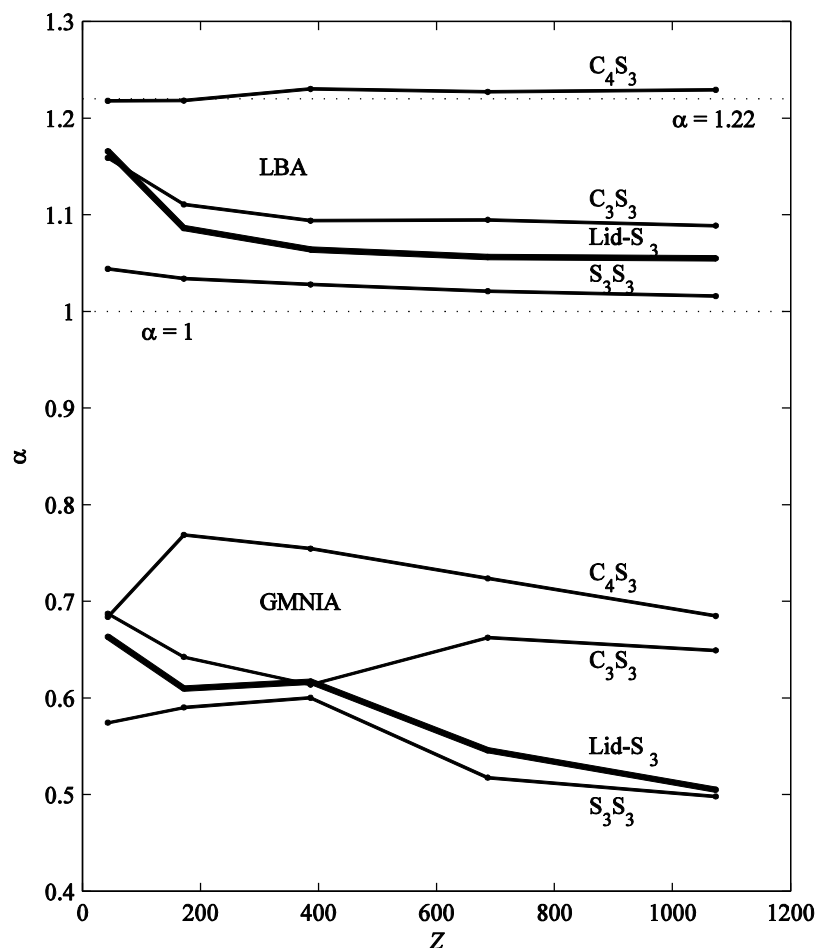

Fig. 9 Buckling load for various boundary conditions. Top group: LBA, bottom group: GMNIA

4. Partially embedded cylinder—Influence of soil–structure interaction

The lid is considered pinned in order to isolate the influence from embedding the cylinder in an elastic soil. Fig. 10(a) shows the effect of penetration ratio on the buckling load normalised with respect to the elastic buckling load of a pinned cylinder with length equal to the total length of the embedded cylinder ($l = L$) and also defining Z (≈ 1100) in terms of the total length, L. As expected, the penetration ratio has a significant influence on the buckling load. As the penetration ratio is increased, the buckling load increases more than linearly. In Fig. 10(b) is shown the ratio between the GMNIA and the LBA buckling load, also known as the knockdown factor. For a tie constraint between the cylinder and the surrounding soil, the knockdown factor is approximately 0.6. Allowing lateral separation and introducing Coulomb friction reduces the knockdown factor to approximately 0.5 for higher penetration ratios. The values for $\mu = 20$ and 0.42 are almost identical, meaning that the reduction compared to the tie constraint is mainly due to allowing separation. Fig. 11 shows an image at collapse illustrating separation for $\mu = 20$ and 0.42.

In Fig. 12(a) the buckling load of the partially submerged cylinder is normalised with respect to the elastic buckling load of a pinned–pinned (S_3S_3) cylinder of height equal to the free height, for the case of Z (based on $l = L$) ≈ 1100. The LBA values indicate that the elastic buckling load of the partially submerged cylinder is approximately 10% larger than for a simply supported cylinder of height equal to the free height of the partially submerged cylinder. This indicates that the cylinder is partially clamped at the seabed. The nonlinear buckling load of a partially submerged cylinder with tie constraints is approximately 0.65 of the elastic buckling load of a simply supported cylinder of height equal to the free height of the partially submerged cylinder. As observed in Fig. 10(b), modelling the soil–structure interface more accurately yields lower nonlinear buckling loads than using tie constraints. This difference is more pronounced for larger penetration ratios.
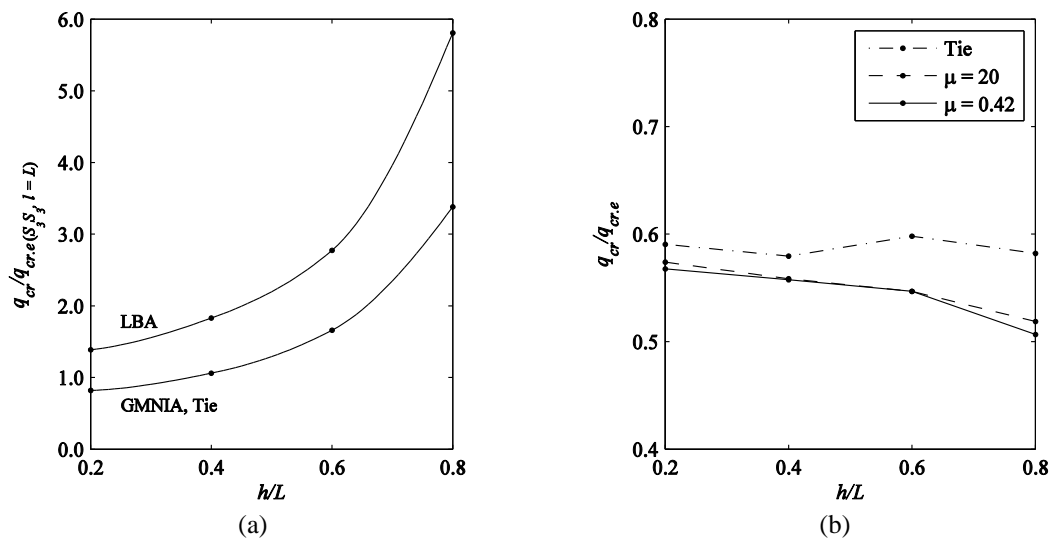

Fig. 10 Buckling load for various penetration ratios. $Z \approx 1100$. Left (a): Normalised with respect to elastic buckling load of a S_3S_3 cylinder of length equal to the total height. Right (b): Knockdown factor (GMNIA / LBA). Hydrostatic load. S_3 - soil. $E_{soil} = 25$ MPa
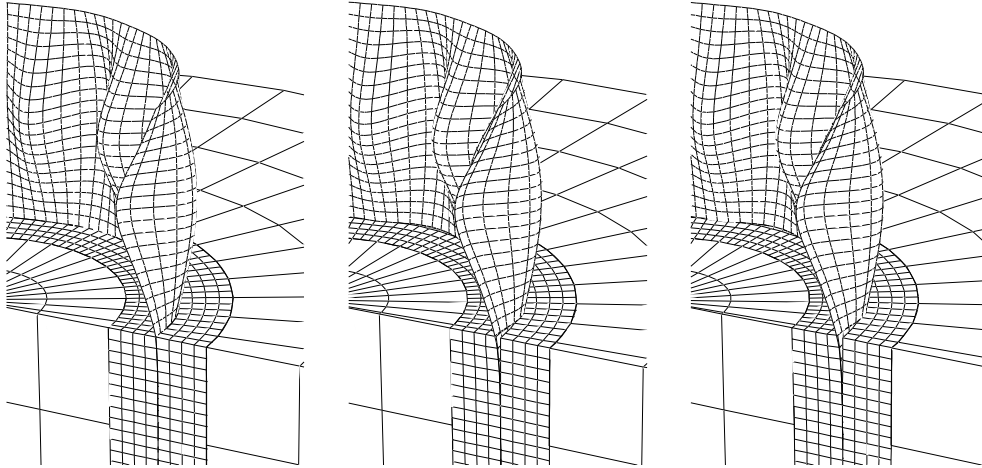
Fig. 11 Section through mesh at collapse load where separation can be seen for $\mu = 20$ and 0.42. Left to right: Tie, $\mu = 20$ and 0.42. Deformations scaled 25 times
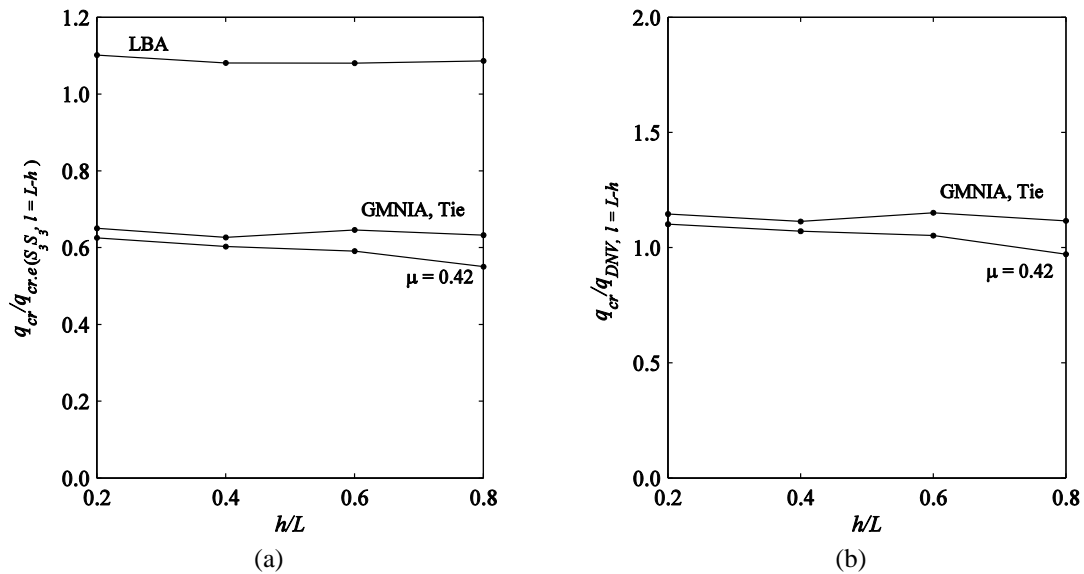

Fig. 12 Buckling load normalised with respect to elastic buckling load of a S_3S_3 cylinder of length equal to the free height (a) and DNV solution (b). Hydrostatic load. S_3–soil. $E_{soil} = 25$ MPa.

From Fig. 12(b), where the nonlinear buckling load is normalised with respect to the DNV solution for a cylinder of length equal to the free height, it is seen that when adding 10–15% to the DNV solution it matches the buckling load obtained by nonlinear numerical analysis when considering tie constraints quite well for all penetration ratios. This is also the case for low

penetration ratios when considering tangential sliding and allowing lateral separation. For a penetration ratio of 0.8, the numerical result matches the DNV solution. This indicate that for initial penetration the soil represents a higher fixity than the pinned case used in the DNV.

5. Design recommendations

Several factors must be considered when designing monopod bucket foundations against buckling: Boundary conditions, geometrical imperfections, soil restraint.

- For initial design, the buckling load may be calculated for varying cylinder lengths—corresponding to the free cylinder height—using S_3S_3 boundary conditions and applying a knockdown factor to account for imperfections. These results should be compared to the required installation pressure.
- For detailed design, a similar analysis could be carried out or a full finite element analysis may be conducted. If the latter, the effect of soil restraint is worth considering—especially if weaker soils than considered in this paper are present.

6. Conclusions

In this paper, the effect on the buckling load of modelling the real bucket lid was compared to idealized boundary conditions. The bucket lid shows an increase in the buckling load compared to a pinned end, especially for shorter cylinders. The number of stiffeners on the lid does not substantially affect the elastic buckling load. An unrealistically thick lid would be required to obtain a clamped solution. Conservatively, the lid end could be considered pinned.

Further, the influence of soil–structure interaction on the buckling load was investigated. The soil restraint increases the buckling load significantly when penetrating the cylinder. Including tangential sliding and allowing lateral separation decreases the buckling load of the partially submerged cylinder compared to using tie constraints. The main contribution to this decrease is allowing lateral separation. For practical applications, the DNV solution could be used when the cylinder length is set equal to the free height of the partially submerged cylinder.

References

Andersen, K.H., Jostad, H.P. and Dyvik, R. (2008), "Penetration resistance of offshore skirted foundations and anchors in dense sand", *J. Geotech. Geoenviron. Eng.*, **134**(1), 106-116.

Andersen, L. (2010), "Assessment of lumped-parameter models for rigid footings", *Comput. Struct.*, **88**(23-24), 1333-1347.

Arbocz, J. (1982), *The imperfection data bank, a mean to obtain realistic buckling loads*, in *Buckling of Shells*, Stuttgart, May.

Brush, D. and Almroth, B. (1975), *Buckling of Bars, Plates and Shells*, McGraw-Hill, New York.

Bushnell, D. (1981), "Buckling of shells - pitfall for designers", *AIAA J.*, **19**(9), 1183-226.

DNV-RP-C202 (2013), *Recommended practice: Buckling strength of shells*, Det Norske Veritas.

EN 1993-1-6 (2007), *Eurocode 3 - Design of steel structures - Part 1-6: Strength and Stability of Shell Structures*.

Farshad, M. (1992), *Design and Analysis of Shell Structures*, Kluwer Academic Publishers, The

Netherlands.

Guggenberger, W. (1995), "Buckling and post–buckling of imperfect cylindrical shells under external pressure", *Thin Wall. Struct.*, **23**(1-4), 351-366.

Hanssen, S.B, Giese, S., Bye, A, Athanasiu, C. and Tistel, J. (2013), "Modeling of lateral soil restraint for buckling analysis of suction caissons in clay", *Proceedings of the 23rd Int Offshore and Polar Eng Conf,* Anchorage, Alaska, USA, June-July.

Haynie, W.T. and Hilburger, M.W. (2010), "Comparison of methods to predict lower bound buckling loads of cylinders under axial compression", *Proceedings of the 51st AIAA/ASME/ASCE/AHS/ASC Structures, Structural Dynamics, and Materials Conference*, Orlando, Florida, April.

Houlsby, G., Ibsen, L.B. and Byrne, B. (2005), "Suction caissons for wind turbines", in *Frontiers in Offshore Geotechnics: ISFOG 2005*, University of Western Australia, Perth, September.

Hrinda, G.A. (2012), "Effects of shell-buckling knockdown factors in large cylindrical shells", *Proceedings of the 53rd AIAA/ASME/ASCE/AHS/ASC Structures, Structural Dynamics and Materials Conference*, Honolulu, Hawaii, April.

Ibsen, L.B. (2008), "Implementation of a new foundations concept for offshore wind farms", *Proceedings of the Nordisk Geoteknikermøte nr. 15: NGM 2008.* Sandefjord, Norway, September.

Ibsen L.B. and Thilsted C.L. (2010), "Numerical study of piping limits for suction installation of offshore skirted foundations an anchors in layered sand", in *Frontiers in Offshore Geotechnics II: proceedings of the 2nd international symposium on frontiers in offshore geotechnics*, Perth, Australia, November.

Lee, G.H. and Tran, D.P. (2013), "Buckling behaviors of bucket foundation for offshore wind tower", *J. Korean Soc, Coastal Ocean Engineers*, **25**(3), 123-127.

Lesny, K. (2010), *Foundations for offshore wind turbines: tools for planning and design*, VGE Verlag GmbH, Essen, Germany.

Madsen, S., Andersen, L. and Ibsen, L.B. (2013), "Numerical buckling analysis of large suction caissons for wind turbines on deep water", *Eng. Struct.*, **57,** 443-452.

NASA (1968), *Buckling of thin-walled circular cylinders*, NASA SP-8007.

Noor, A.K. (1992), "Bibliography of monographs and surveys on shells", *Appl. Mech. Rev.*, **43**(9), 223-234.

Odland, J. (1981), *On the strength of welded ring stiffened cylindrical shells primarily subjected to axial compression*, Technical Report UR-81-15, Division of Marine Structures, The University of Trondheim, The Norwegian Institute of Technology.

Odland, J. and Faulkner, D. (1981), *Buckling of curved steel structures - design formulations*, Integrity of Offshore Structures, Applied Science Publishers.

de Paor, C., Kelliher, D., Cronin, K., Wright, W.M.D. and McSweeney, S.G. (2012), "Prediction of vacuum-induced buckling pressures of thin-walled cylinders", *Thin Wall. Struct.*, **55**, 1-10.

Pinna, R. and Ronalds, B.F. (2000), "Hydrostatic buckling of shells with various boundary conditions", *J. Constr. Steel Res.*, **56**(1), 1-16.

Pinna, R., Martin, C. and Ronalds, B. (2001), "Guidance for design of suction caissons against buckling during installation in clay soils", *Proceedings of the 11th International Offshore and Polar Engineering Conference*, Stavanger, Norway. June.

Pinna, R. (2004), *Buckling of suction caissons during installation*, Ph.D. Dissertation, University of Western Australia, Perth.

Prabu, B., Rathinam, N., Srinivasan, R. and Naarayen, K.A.S. (2009), "Finite element analysis of buckling of thin cylindrical shell subjected to uniform external pressure", *Journal of Solid Mechanics,* **1**(2), 148-158.

Schmidt, H. (2000), "Stability of steel shell structures: General report", *J. Constr. Steel Res.*, **55**(1-3), 159-181.

Simitses, G.J. (1986), "Buckling and postbuckling of imperfect cylindrical shells", *Appl. Mech. Rev.*, **39**(10), 1517-1524.

Sofiyev, A. (2010), "Buckling analysis of fgm circular shells under combined loads and resting on the Pasternak type elastic foundation", *Mech. Res. Commun.*, **37**(6), 539-544.

Teng. J.G. (1996), "Buckling of thin shells: Recent advances and trends", *Appl. Mech. Rev.*, **49**(4), 263-274.

Tjelta, T.I. (1995), "Geotechnical experience from the installation of the Europipe jacket with bucket foundations", *Proceedings of the Offshore Technology Conference (OTC)*, Houston, Texas, U.S.A., May.

Tran, M.N. and Randolph, M.F. (2008), "Variation of suction pressure during caisson installation in sand", *Géotechnique*, **58** (1), 1-11.